

~~CONFIDENTIAL~~

RM A51H10a

CLASSIFICATION CHANGED

OCT 18 1951

C.2

~~RESTRICTED~~

To:

~~RESTRICTED~~~~CONFIDENTIAL~~~~CONFIDENTIAL~~
SECURITY INFORMATION

RESEARCH MEMORANDUM

TESTS IN THE AMES 40- BY 80-FOOT WIND TUNNEL OF AN AIRPLANE

CONFIGURATION WITH AN ASPECT RATIO 4 TRIANGULAR WING

AND AN ALL-MOVABLE HORIZONTAL TAIL -

LONGITUDINAL CHARACTERISTICS

By David Graham and David G. Koenig

Ames Aeronautical Laboratory
Moffett Field, Calif.

CLASSIFIED DOCUMENT

This document contains classified information affecting the National Defense of the United States within the meaning of the Espionage Act, USC 5031 and 32. Its transmission or the revelation of its contents in any manner to an unauthorized person is prohibited by law.

Information so classified may be imparted only to persons in the military and naval services of the United States, appropriate civilian officers and employees of the Federal Government who have a legitimate interest therein, and to United States citizens of known loyalty and discretion who of necessity must be informed thereof.

NATIONAL ADVISORY COMMITTEE
FOR AERONAUTICSWASHINGTON
October 16, 1951NATIONAL ADVISORY
LANGLEY AERONAUTICAL LABORATORY
Langley Field, Va.~~CONFIDENTIAL~~~~CONFIDENTIAL~~
SECURITY INFORMATION

NACA RM A51H10a

CLASSIFICATION CANCELLED

Authority NACA 124-3-1-1 Date 8/17/53

By DA2474-8/31/53-1

See

CLASSIFICATION CHANGED

Confidential

By authority of J. H. C. 124-3-1-1 Date 12/11/53

NACA RM A51H10a 12/11/53

~~CONFIDENTIAL~~~~CONFIDENTIAL~~
~~SECURITY INFORMATION~~

NATIONAL ADVISORY COMMITTEE FOR AERONAUTICS

RESEARCH MEMORANDUM

TESTS IN THE AMES 40- BY 80-FOOT WIND TUNNEL OF AN AIRPLANE

CONFIGURATION WITH AN ASPECT RATIO 4 TRIANGULAR WING

AND AN ALL-MOVABLE HORIZONTAL TAIL -

LONGITUDINAL CHARACTERISTICS

By David Graham and David G. Koenig

SUMMARY

An investigation has been made to determine the low-speed longitudinal characteristics of an aspect ratio 4 triangular wing, alone and in combination with a fuselage, vertical tail, and horizontal tail. The complete model consisted of the wing (NACA 0005 modified airfoil section) in combination with a fuselage of fineness ratio 12.5; a thin, triangular, vertical tail; and each of two thin, unswept, all-movable horizontal tails (aspect ratios of approximately 2 and 4). Tests were made with the horizontal tails at each of three vertical distances above the wing-chord plane (0, 0.18, and 0.36 wing semispan) at one longitudinal distance behind the wing. The average Reynolds number, based on the wing mean aerodynamic chord, was 10.9×10^6 and the Mach number was 0.13.

The results of the investigation showed that the model with either tail located in the extended wing-chord plane had a stabilizing variation of the aerodynamic center position with lift coefficient throughout the lift range; whereas there were large destabilizing variations of the aerodynamic center position for the model with either tail located in the positions above the wing-chord plane. This effect of vertical position of the horizontal tail on the longitudinal stability is similar to that obtained for a configuration with an aspect ratio 2 triangular wing (NACA RM A51B21, 1951).

INTRODUCTION

The results of tests of an aspect ratio 4 triangular wing (reference 1) have shown the wing to be suitable for use at supersonic speeds.

~~CONFIDENTIAL~~~~CONFIDENTIAL~~
~~SECURITY INFORMATION~~

In order to determine the aerodynamic characteristics of a similar wing at large scale and low speed, an investigation has been conducted in the Ames 40- by 80-foot wind tunnel.

The results of reference 1 with regard to aerodynamic-center shift and of reference 2 with regard to damping in pitch indicate that prime consideration should be placed on the use of the wing in an airplane configuration with a horizontal tail. Therefore tests were conducted to determine the low-speed longitudinal characteristics of an airplane configuration with the aspect ratio 4 triangular wing and a horizontal tail. The results of tests reported in reference 3 showed that the vertical position of a horizontal tail had a marked effect on the longitudinal stability of a model with an aspect ratio 2 wing; hence the vertical position of the tail was varied in the present case. In addition, the effect of a variation of tail span on the longitudinal stability was investigated.

NOTATION

- A wing aspect ratio $\left(\frac{b^2}{S}\right)$
- A_t horizontal tail aspect ratio $\left(\frac{b_t^2}{S_t}\right)$
- α angle of attack of the wing-chord plane with reference to free stream, degrees
- b wing span, feet
- b_t horizontal-tail span, feet
- c wing chord, measured parallel to wing center line, feet
- \bar{c} mean aerodynamic chord of wing measured parallel to wing center line $\left(\frac{\int_0^{b/2} c^2 dy}{\int_0^{b/2} c dy}\right)$, feet
- C_D drag coefficient $\left(\frac{D}{qS}\right)$
- C_L lift coefficient $\left(\frac{L}{qS}\right)$

- C_m pitching-moment coefficient $\left(\frac{M}{qSc} \right)$
- D total drag, pounds
- ϵ_{av} average effective downwash angle, degrees
- i_t angle of incidence of the horizontal tail relative to the wing-chord plane, degrees
- l_t distance from center of gravity to pivot line of horizontal tail, feet
- L total lift, pounds
- $\frac{L}{D}$ lift-drag ratio
- M total pitching moment about the center of gravity, foot-pounds
- q free-stream dynamic pressure, pounds per square foot
- S wing area, square feet
- S_t horizontal-tail area, square feet
- W airplane weight, pounds
- y coordinate perpendicular to plane of symmetry, feet
- z coordinate perpendicular to wing-chord plane, feet

APPARATUS AND TESTS

A drawing of the complete airplane model is shown in figure 1 and a photograph of the model in the Ames 40- by 80-foot wind tunnel is shown in figure 2. The pertinent dimensional data are presented in table I. The fuselage, horizontal tail, and vertical tail previously used with an aspect ratio 2 triangular wing (reference 3) were also used for the sub-ject tests.

The wing of the model had an aspect ratio of 4. The airfoil sections parallel to the model center line were modified NACA 0005 sections. The modification consisted of a straight-line fairing from the 67-percent-chord station to the trailing edge. Coordinates of the airfoil are listed in table II.

The fuselage was of circular cross section and had a fineness ratio of 12.5. Coordinates for the fuselage are presented in table III.

Two all-movable horizontal tails were used. Each tail had an unswept plan form and modified diamond sections. The original diamond section of 5.6-percent thickness was modified by rounding the maximum-thickness ridge using a radius of curvature of 4.48 chord; the resulting section had a maximum thickness of 4.2-percent chord. Each horizontal tail was tested at three positions, namely, at the low, middle, and high positions shown in figure 1. Each tail was pivoted about a line connecting the leading edges of its tip sections. In the low position, each horizontal tail was mounted on the fuselage with its pivot line in the extended chord plane of the wing. In the middle and high positions, the horizontal tails were mounted on the vertical tail with the pivot lines located vertically at approximately 18- and 36-percent wing semispan above the wing-chord plane, respectively. (See table I and fig. 1.) The longitudinal location was the same for all three tail positions. The same horizontal-tail surface panels were used at each of the three positions. Tail 1, which was used in the investigation reported in reference 3, had an aspect ratio of 4 when mounted on the vertical tail. The aspect ratios of the tails were larger when at the low position than at the other two positions. (See table I.)

Force and moment data were obtained for the wing alone, wing-fuselage, wing-fuselage-vertical-tail configuration, and the complete model with each horizontal tail at each of the three positions. The tails were set at 0° , -2° , and -6° angle of incidence at each of the three tail positions. With the tails in the low position, additional tests were made at an angle of incidence of -10° . Accuracy of horizontal-tail settings was within $\pm 0.2^\circ$. All tests were made at zero sideslip through an angle-of-attack range of approximately -1° to 24° .

The average Reynolds number of the tests was 10.9 million based on the mean aerodynamic chord of the wing. The dynamic pressure was approximately 25 pounds per square foot and the Mach number was 0.13.

RESULTS

Lift, drag, and pitching-moment data for the wing alone, wing-fuselage, and wing-fuselage-vertical-tail configurations are presented in figure 3. The pitching-moment data in this figure are referred to the quarter-chord station of the mean aerodynamic chord. The lift, drag, and pitching-moment data for the complete model with each of the two horizontal tails are shown in figures 4, 5, and 6. The pitching-moment data in these figures are referred to center-of-gravity locations for which a value

of $(dC_m/dC_L)_{C_L=0} = -0.06$ was obtained with the horizontal tail at $i_t = 0^\circ$. The center-of-gravity locations used are listed in table IV. The data were corrected for wind-tunnel-wall effects and support-strut interference.

The variations of the average effective downwash angle with angle of attack at the position of the horizontal tail were determined from the pitching-moment data of figures 4, 5, and 6 and are presented in figure 7. The values were determined by the relation

$$\epsilon_{av} = \alpha + i_t$$

where the value of α is that at which the tail-on and tail-off pitching-moment curves intersect. In order to obtain points of intersection for tail incidences other than those tested, a linear variation of dC_m/di_t was assumed.

DISCUSSION

Model Configurations Without Horizontal Tail

Theoretical lift, drag, and pitching-moment curves for the wing alone are compared in figure 3 with the corresponding experimental curves; the simplified lifting-surface theory of reference 4 was used. The curves are noted to be in agreement only in the low lift-coefficient range. In this range the lift-curve-slope prediction is excellent; the predicted slope is 0.058 per degree, and the measured slope is 0.057. The drag curve is also predicted with good accuracy. Prediction of the aerodynamic-center location is fair (33 percent instead of 36 percent \bar{c}).

The foregoing agreement between measured and predicted results as regards degree and C_L range is very similar to that noted for thin triangular wings of lower aspect ratio. The limited lift-coefficient range of applicability of the theory has been shown in the case of a thin triangular wing of aspect ratio 2 to be due to a separation-vortex type of flow which first appears near the tip and spreads inboard with increasing angle of attack. (See reference 5 for a description of this type of flow.) Tuft studies of flow over the aspect ratio 4 wing indicate a similar flow condition to be the reason for the limited range of applicability of the theory.

The effect on the force and moment characteristics of the addition of the fuselage, as in the case of an aspect ratio 2 wing (reference 6), was small. The lift-curve slope was increased from 0.057 per degree to 0.059; $C_{L_{max}}$ was increased from 0.96 to 0.99; and the aerodynamic center

was moved forward from 36 to 34 percent of the mean aerodynamic chord. The addition of the vertical tail caused no significant change in lift or moment.

By superposition of wing-alone and fuselage-alone (unpublished data from Ames 40- by 80-foot wind tunnel) pitching-moment characteristics, an aerodynamic center shift of 5.4 percent of the mean aerodynamic chord is predicted, whereas the experimental results show only a 2-percent shift. This indicates a sizable wing-fuselage interference effect on the aerodynamic-center location, an effect which was also found for the aspect ratio 2 wing-fuselage combination (reference 6).

The data for the wing-fuselage-vertical-tail configuration are compared in figure 8 with data for a similar configuration with an aspect ratio 2 wing (reference 3). Though a similar type of flow separation occurred on the two wings, the effect of this type of flow on the lift and pitching-moment characteristics was quite different. On the aspect ratio 4 wing, the start and progression of the flow separation resulted in a continuously decreasing lift-curve slope and a forward shift of the aerodynamic center followed by a large rearward shift near maximum lift. On the aspect ratio 2 wing, it resulted in only a small irregular aerodynamic-center variation and an increased lift-curve slope which remained fairly constant up to the maximum lift coefficient obtained. The maximum lift coefficients of low-aspect-ratio triangular wings are of minor practical significance, it is believed, because of the high angles of attack involved. It is interesting to note, however, that the maximum lift coefficient of the aspect ratio 2 wing (fig. 8) would be considerably higher than that of the aspect ratio 4 wing.

Model Configurations With Horizontal Tail

Longitudinal stability.— Figures 4, 5, and 6 show the effects of vertical location of the horizontal tail and of tail span on the longitudinal stability characteristics of the model. In all cases it can be seen that the vertical location of the tail was the dominant factor. The following comments on the effect of vertical position apply, therefore, to either tail.

With the tail in the low position, the longitudinal stability increased gradually with increasing lift coefficient until at lift coefficients above 0.8 there was a very rapid increase in stability. With the tail located in the positions above the extended wing-chord plane, the model stability varied widely through the lift range. With the tail in either the middle or high positions, the stability decreased slightly up to lift coefficients of the order of 0.6; then between lift coefficients

of 0.6 and 0.9 there was a large decrease in stability (0.61c and 1.41c forward shift of the aerodynamic center for the middle and high positions, respectively) which was finally followed by a large increase in stability at higher lift coefficients.

The variations of downwash angle with angle of attack (fig. 7), which cause the changes in stability, are believed to be a result of the separation-vortex type of flow. These variations are similar to those obtained on an airplane model with an aspect ratio 2 triangular wing (reference 3). The effect of the separation-vortex type of flow on $d\epsilon_{av}/d\alpha$ and thus the stability contribution of a tail is discussed in reference 3.

As noted in reference 3, downwash surveys show that a horizontal tail at positions slightly above the extended wing-chord plane would be satisfactory for the model with the aspect ratio 2 wing. Since the variations of the downwash angle with angle of attack behind the aspect ratio 4 and aspect ratio 2 wings are similar for corresponding tail positions, the assumption probably can be made that the use of a horizontal tail in positions slightly above the extended wing-chord plane would also be satisfactory for the configuration with the aspect ratio 4 wing.

A comparison of the downwash curves obtained with tails 1 and 2 indicate that, although there are changes in the effective downwash angle at a given angle of attack, the change of tail span does not alter the general variation of the effective downwash angle with angle of attack. Hence, as noted previously, the variation of tail span had only a minor effect on the longitudinal-stability characteristics.

Trim characteristics.— Presented in figure 9 are the lift and drag characteristics for the trimmed airplane with either tail located in the extended wing-chord plane. These characteristics were derived from the data of figure 4. Curves of constant gliding and sinking speeds, computed for a wing loading of 30 pounds per square foot, are included in the figure. Also shown are the lift and drag characteristics of the trimmed airplane configuration with an aspect ratio 2 wing. A 6-percent static margin was assumed for all the airplane configurations. A comparison of the lift and drag characteristics of the two trimmed airplane models indicates, as might be expected, that the airplane with the aspect ratio 4 wing would have better lift and drag characteristics. This is a result of the higher lift-curve slope and lower induced drag of the aspect ratio 4 wing. Hence, the airplane model with this wing is able to attain both lower gliding and sinking speeds, at a given attitude up to an angle of attack of approximately 22° , than the airplane model with the aspect ratio 2 wing. This is shown more clearly in figure 10 where the gliding and sinking speeds of the models with the aspect ratio 2 and 4 wings and tail 1 are plotted as a function of angle of attack. The airplane with the aspect ratio 2 wing, however, is able to attain higher lift coefficients and would thus have

lower minimum gliding speeds if no limitations were placed on maximum permissible attitude, or sinking speed. Before any final conclusions can be drawn, however, the effect of flaps must be determined.

CONCLUDING REMARKS

The results of the investigation showed that the model with either tail located in the extended wing-chord plane had a stabilizing variation of the aerodynamic-center position with lift coefficient throughout the lift range; whereas for the model with either tail located in either of the positions above the wing-chord plane there were large destabilizing variations of the aerodynamic center position.

This effect of vertical position of the horizontal tail on the longitudinal stability has also been found for a configuration with an aspect ratio 2 triangular wing (NACA RM A51B21, 1951). It is believed that the same effect can, therefore, be expected for airplane models having thin triangular wings with aspect ratios between 2 and 4.

Ames Aeronautical Laboratory,
National Advisory Committee for Aeronautics,
Moffett Field, Calif.

REFERENCES

1. Heitmeyer, John C., and Stephenson, Jack D.: Lift, Drag, and Pitching Moment of Low-Aspect-Ratio Wings at Subsonic and Supersonic Speeds - Plane Triangular Wing of Aspect Ratio 4 with NACA 0005-63 Section. NACA RM A50K24, 1951.
2. Tobak, Murray, Reese, David E., Jr., and Beam, Benjamin H.: Experimental Damping in Pitch of 45° Triangular Wings. NACA RM A50J26, 1950.
3. Graham, David, and Koenig, David G.: Tests in the Ames 40- by 80-Foot Wind Tunnel of an Airplane Configuration with an Aspect Ratio 2 Triangular Wing and an All-Movable Horizontal Tail - Longitudinal Characteristics. NACA RM A51B21, 1951.
4. DeYoung, John, and Harper, Charles W.: Theoretical Symmetric Span Loading at Subsonic Speeds for Wings Having Arbitrary Plan Form. NACA Rep. 921, 1948.

5. Anderson, Adrien E.: Chordwise and Spanwise Loadings Measured at Low Speeds on Large Triangular Wings. NACA RM A9B17, 1949.
6. Anderson, Adrien E.: An Investigation at Low Speed of a Large-Scale Triangular Wing of Aspect Ratio Two.-III. Characteristics of Wing with Body and Vertical Tail. NACA RM A9H04, 1949.

TABLE I.— DIMENSIONAL DATA

Wing			
Area, square feet			312.5
Span, feet			35.36
Mean aerodynamic chord, feet			11.78
Aspect ratio			4.0
Taper ratio			0
Fuselage			
Length, feet			56.16
Maximum diameter, feet			4.49
Fineness ratio			12.5
Vertical tail			
Exposed area, square feet			52.57
Aspect ratio of plan form, extended to model center line			1
Taper ratio			0
Airfoil section parallel to model center line			Modified NACA 0005
Horizontal tail			
Low position	<u>Tail 1</u>	<u>Tail 2</u>	
S_t/S	0.246	0.266	
b_t/b	0.521	0.391	
l_t/\bar{c}	1.735	1.752	
Aspect ratio	4.4	2.3	
Taper ratio	0.46	0.45	
Middle position			
S_t/S	0.200	0.200	
b_t/b	0.448	0.316	
l_t/\bar{c}	1.703	1.750	
Aspect ratio	4.0	2.0	
Taper ratio	0.50	0.50	

TABLE I.- CONCLUDED

High position	<u>Tail 1</u>	<u>Tail 2</u>
s_t/s	0.200	0.200
b_t/b	0.448	0.316
z_t/c	1.679	1.733
Aspect ratio	4.0	2.0
Taper ratio	0.50	0.50

NACA

TABLE II.— COORDINATES OF THE NACA 0005
(MODIFIED) SECTION

Station (percent chord)	Ordinate (percent chord)
0	0
1.25	.789
2.50	1.089
5.00	1.481
7.50	1.750
10.00	1.951
15.00	2.228
20.00	2.391
25.00	2.476
30.00	2.501
40.00	2.419
50.00	2.206
60.00	1.902
67.00	1.650
70.00	1.500
80.00	1.000
90.00	.500
100.00	0
L.E. radius, 0.275-percent chord	



TABLE III.— BODY COORDINATES

[Stations and radii in percent
of the total length]

Station		Radius
0	100.00	0
.625	99.375	.26
1.25	98.75	.42
2.50	97.50	.70
5.00	95.00	1.15
7.50	92.50	1.54
10.00	90.00	1.86
15.00	85.00	2.41
20.00	80.00	2.86
25.00	75.00	3.22
30.00	70.00	3.51
35.00	65.00	3.73
40.00	60.00	3.88
45.00	55.00	3.97
50.00	— — —	4.00



TABLE IV.— CENTER-OF-GRAVITY LOCATIONS
FOR THE VARIOUS CONFIGURATIONS

Configuration	Center-of-gravity location (percent \bar{c})
Wing alone	25.0
Wing-fuselage	25.0
Wing-fuselage-vertical-tail ¹	25.0
Complete model with tail 1	
Low	40.8
Middle	43.9
High	46.3
Complete model with tail 2	
Low	39.0
Middle	39.3
High	41.0

¹In figures 4, 5, and 6, where the wing-fuselage-vertical-tail-configuration data are compared with the data for the complete model, the center-of-gravity location for the complete model is used.



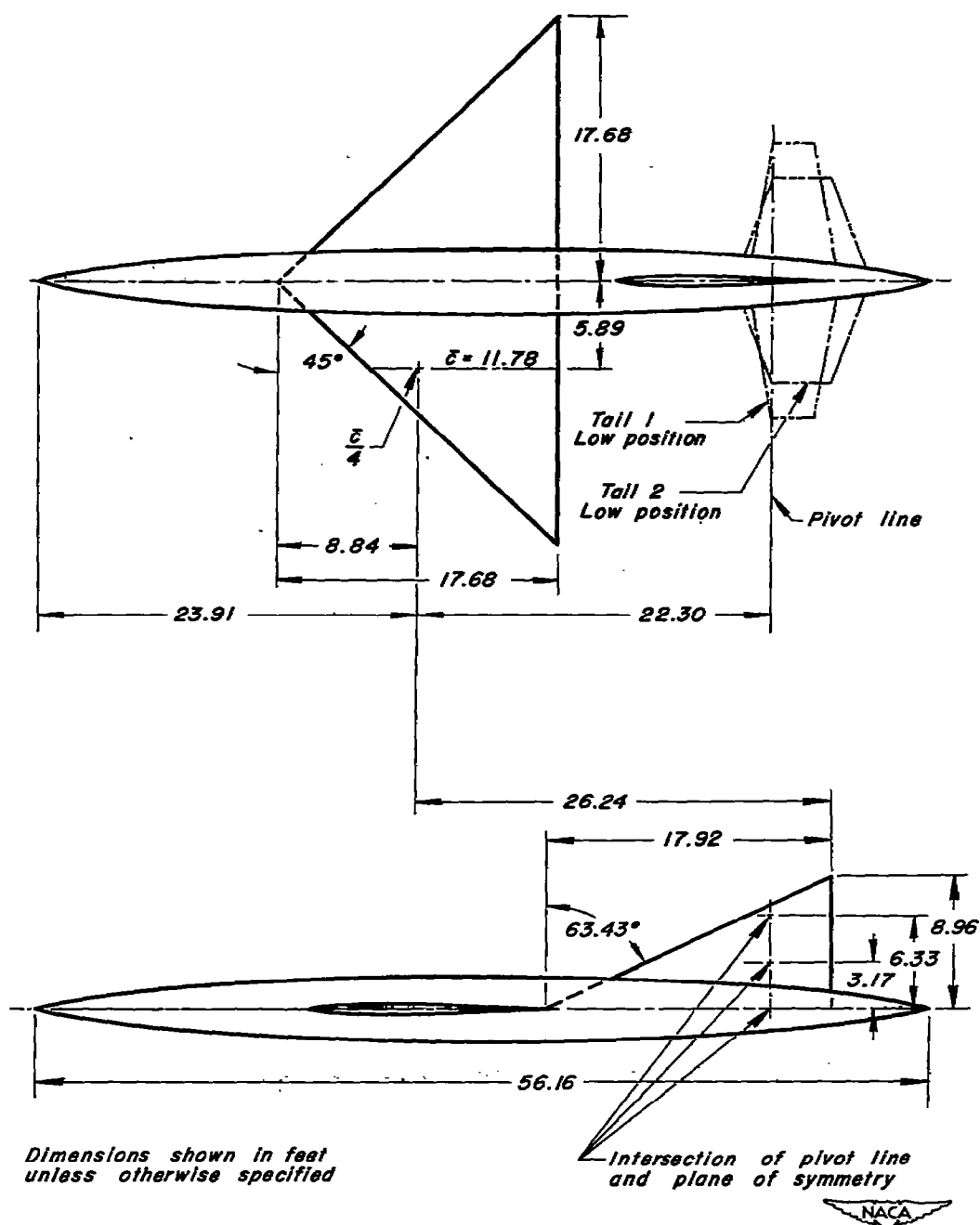


Figure 1.- Geometric details of the model.

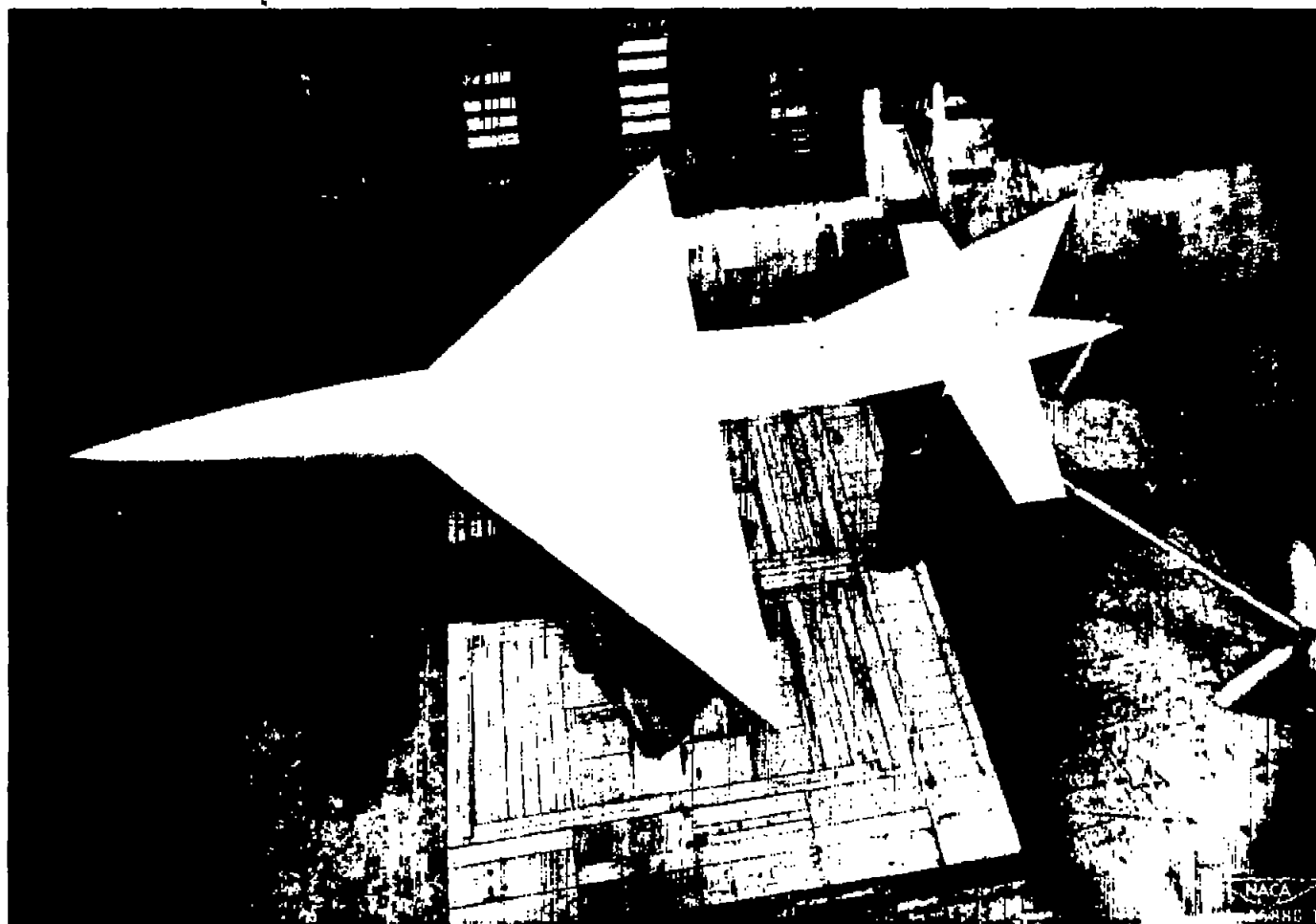


Figure 2.- The model as mounted in the Ames 40- by 80-Foot Wind Tunnel.
Horizontal tail 1 in low position.

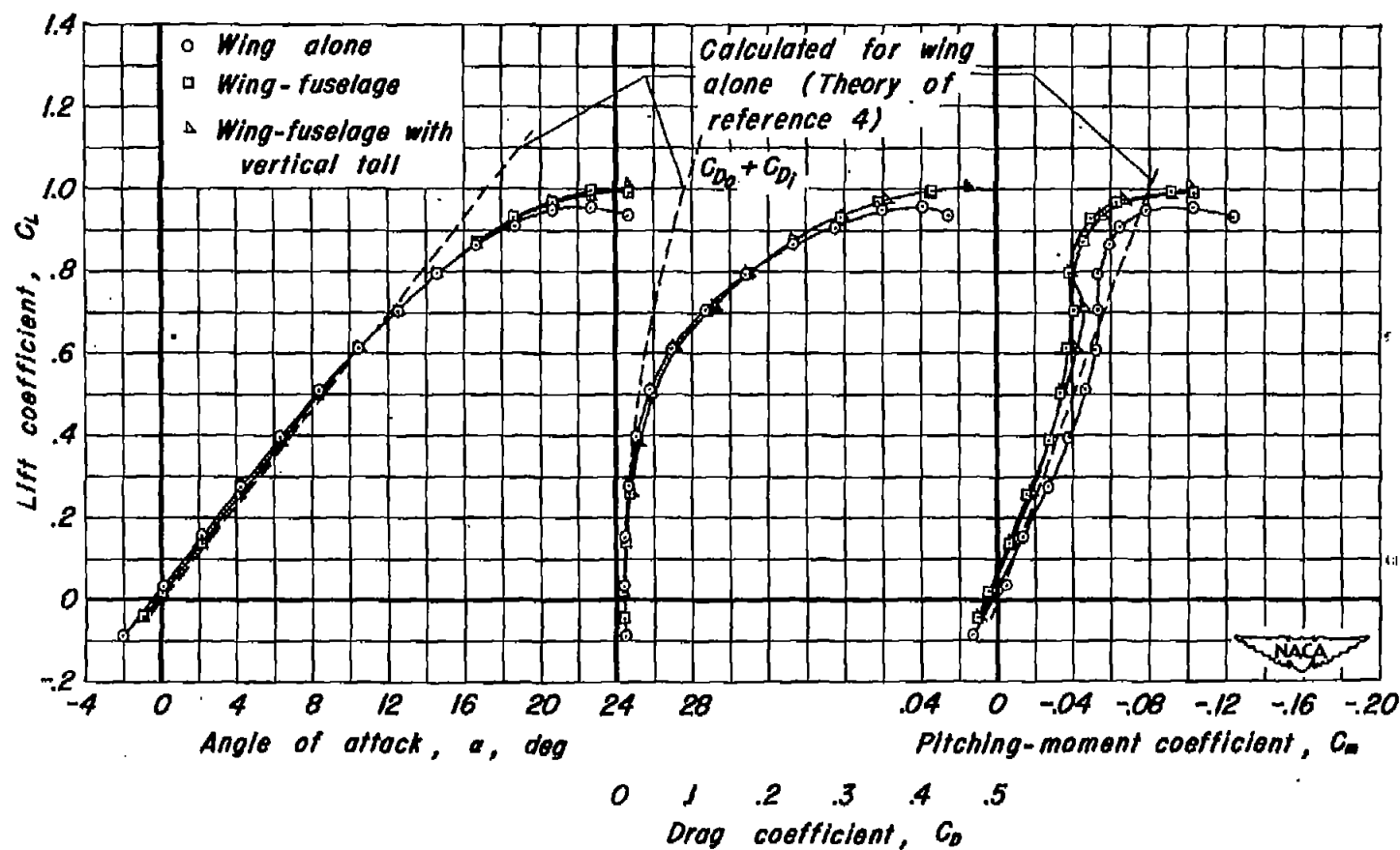
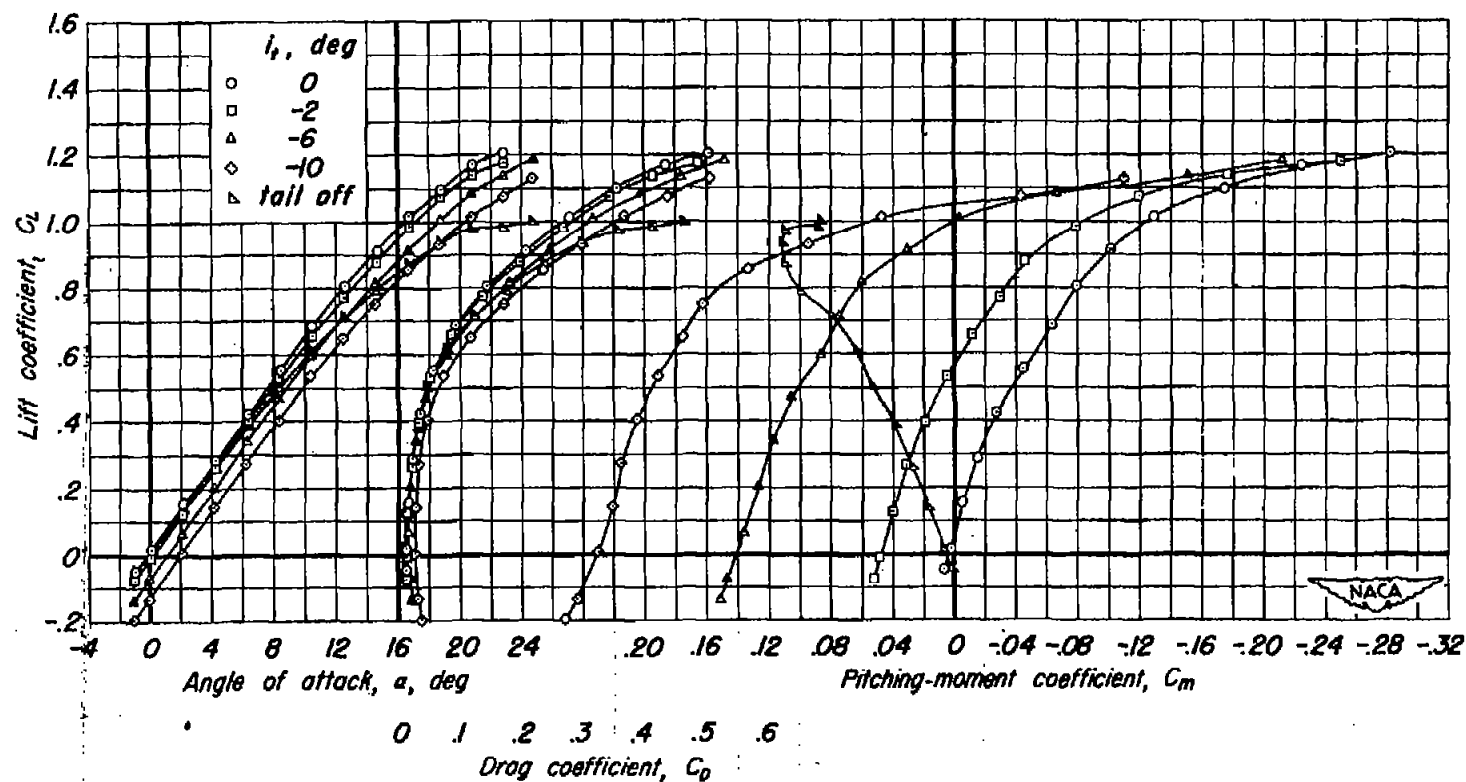
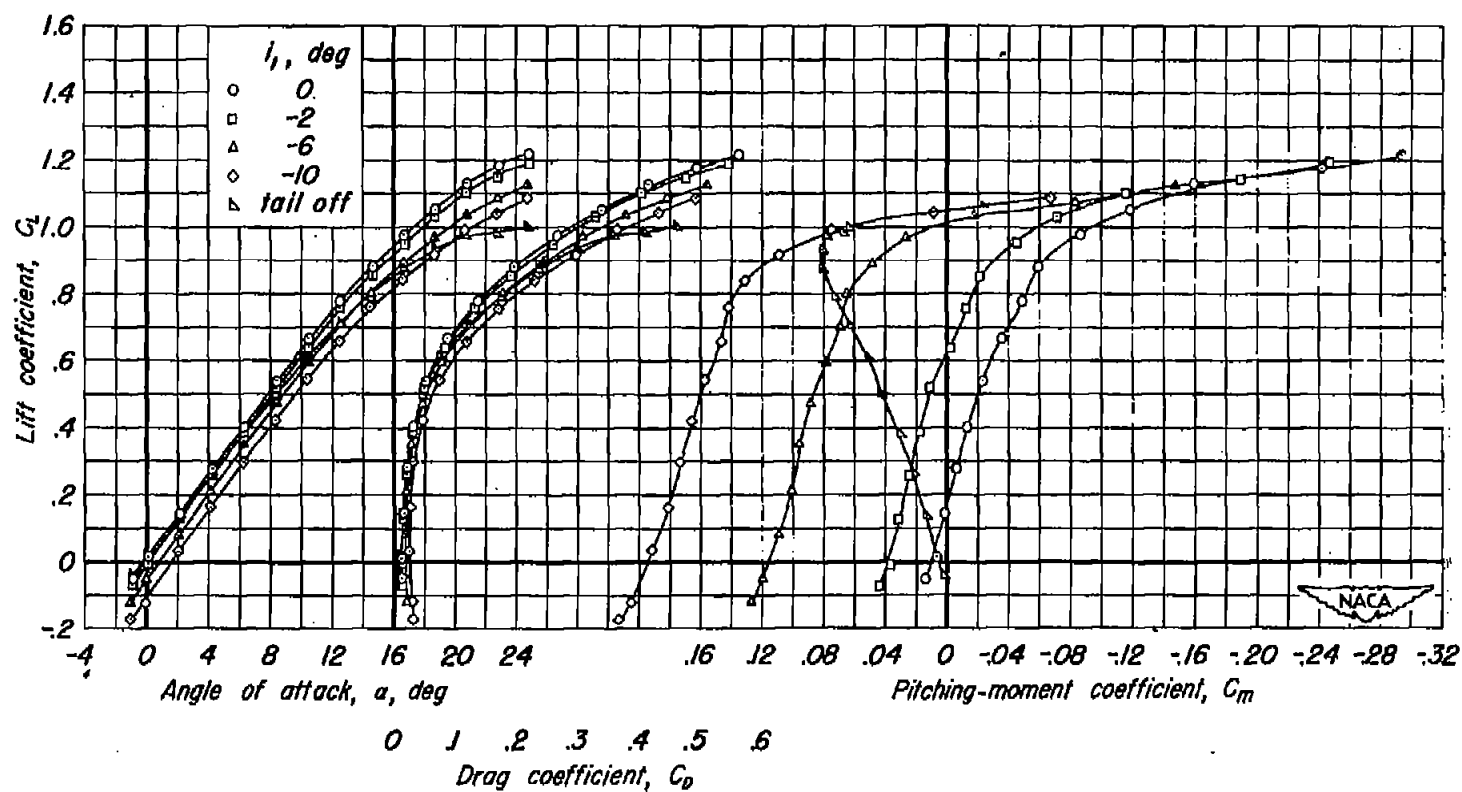


Figure 3.- Aerodynamic characteristics of the wing-alone, wing-fuselage, and wing-fuselage-vertical-tail configurations; c.g., 0.250 \bar{c} .



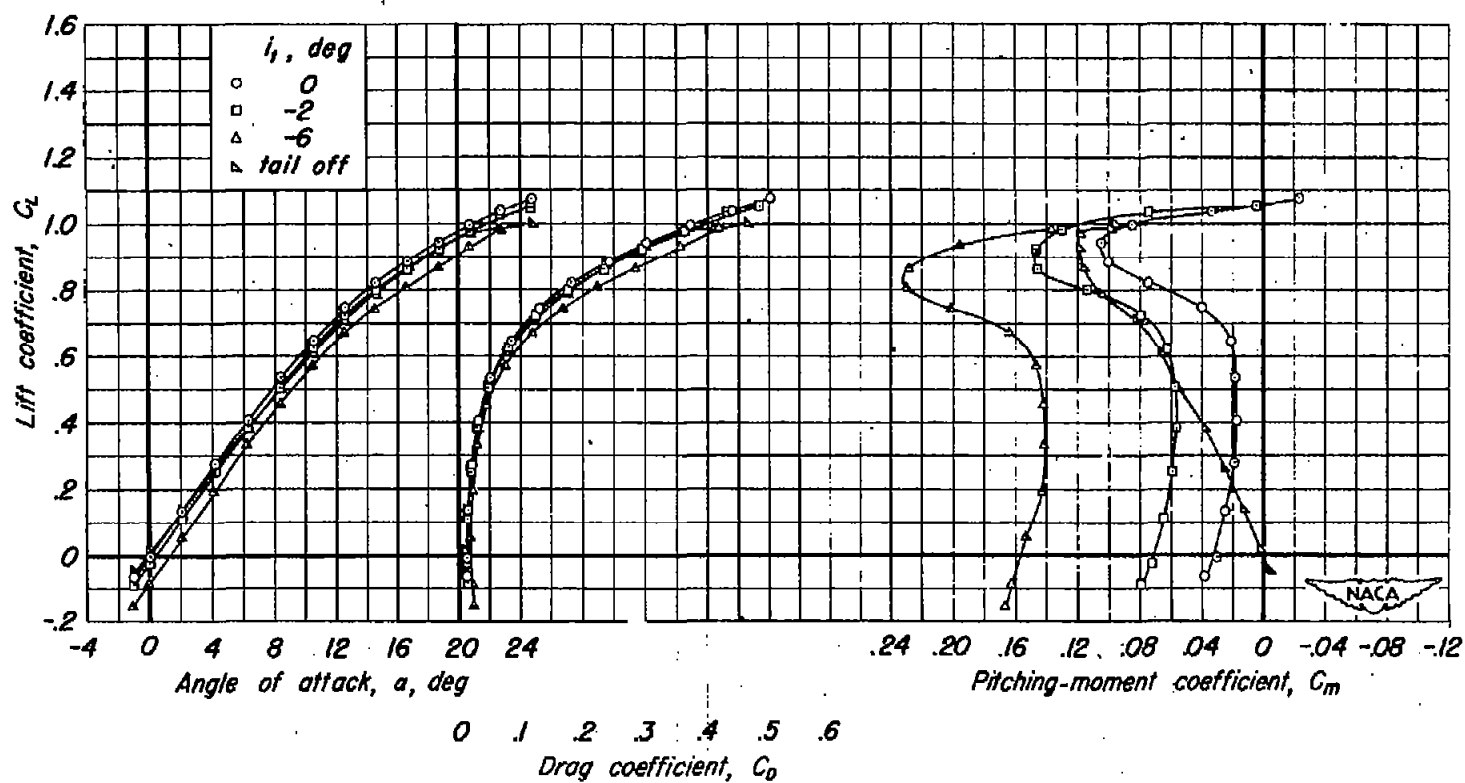
(a) Tail I; c.g., 0.408 \bar{c} .

Figure 4. Longitudinal characteristics of the model with the horizontal tails in the low position. $\frac{z}{b/2}$, 0.



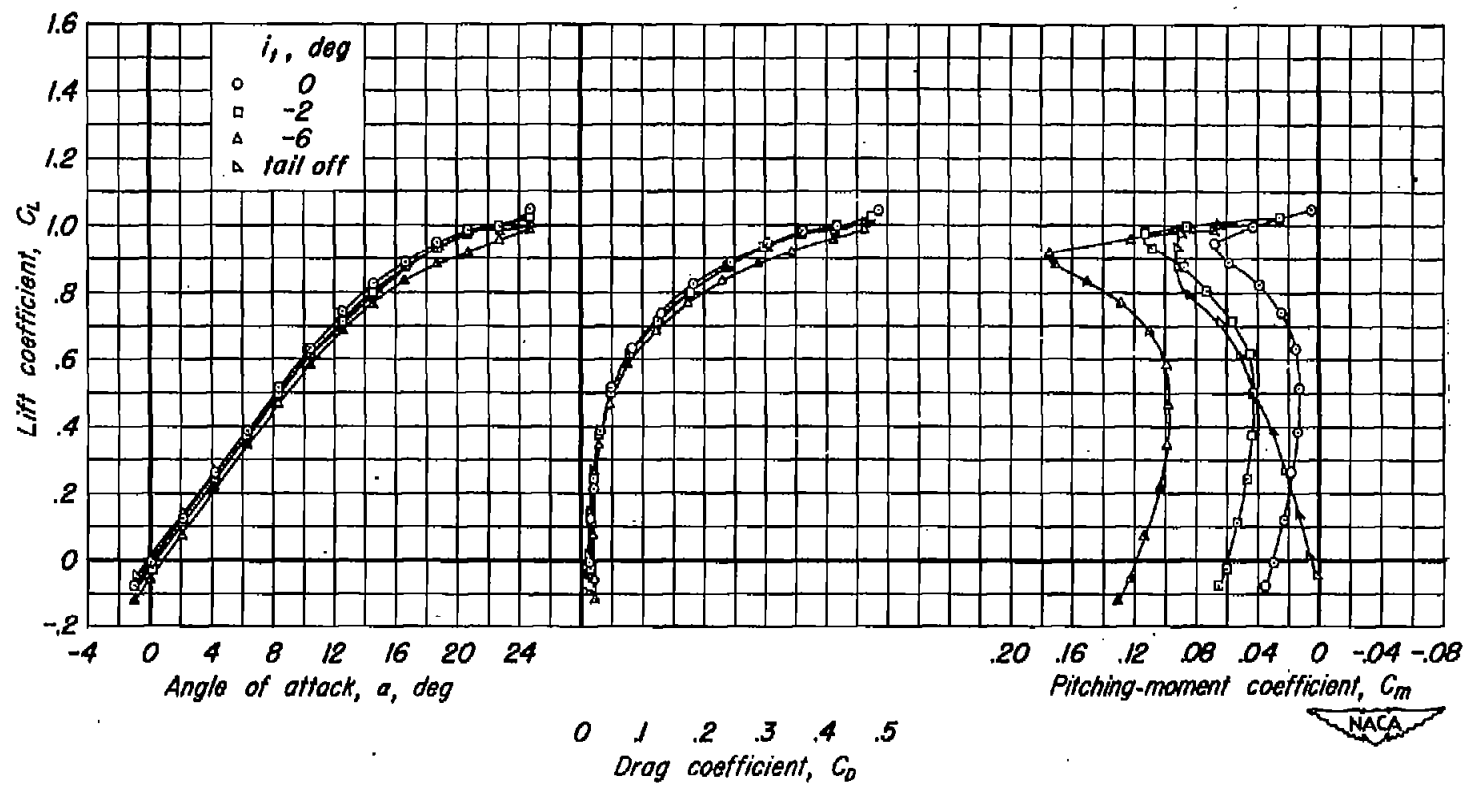
(b) Tail 2; c.g., 0.390 \bar{c} .

Figure 4.- Concluded.



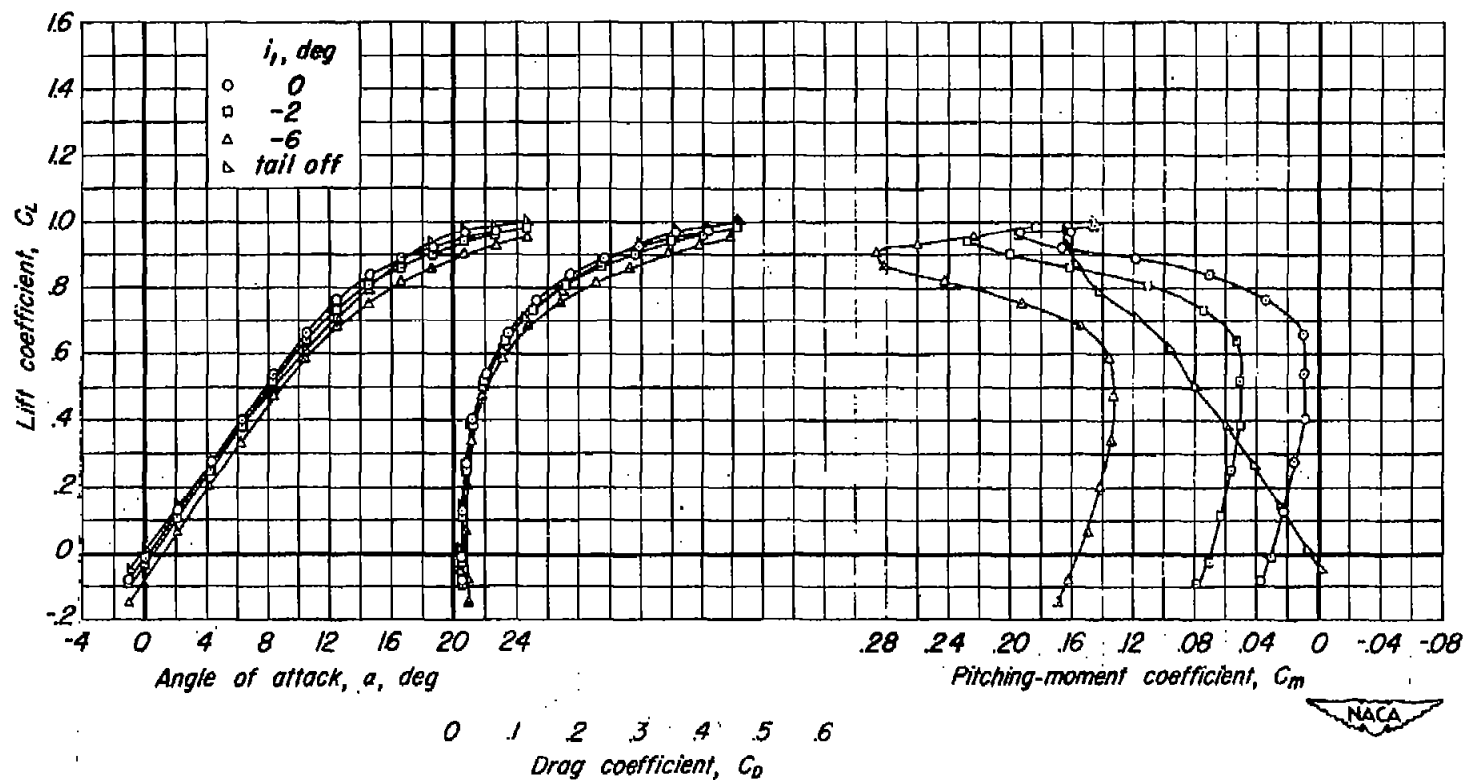
(a) Tail I; c.g., 0.439 \bar{c} .

Figure 5.- Longitudinal characteristics of the model with the horizontal tails in the middle position, $\frac{z}{b/2}$, 0.18.



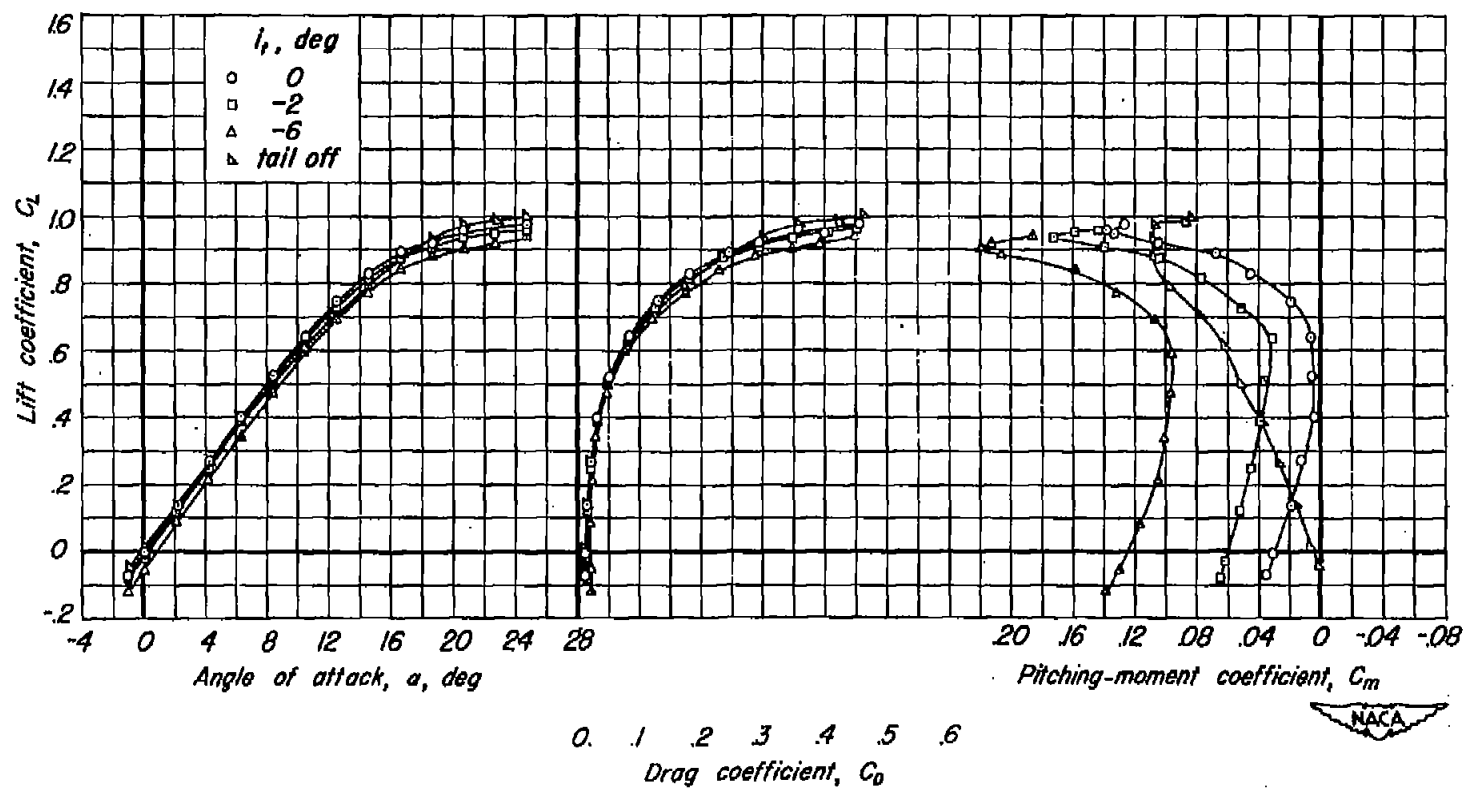
(b) Tail 2; c.g., 0.393 c.

Figure 5- Concluded.



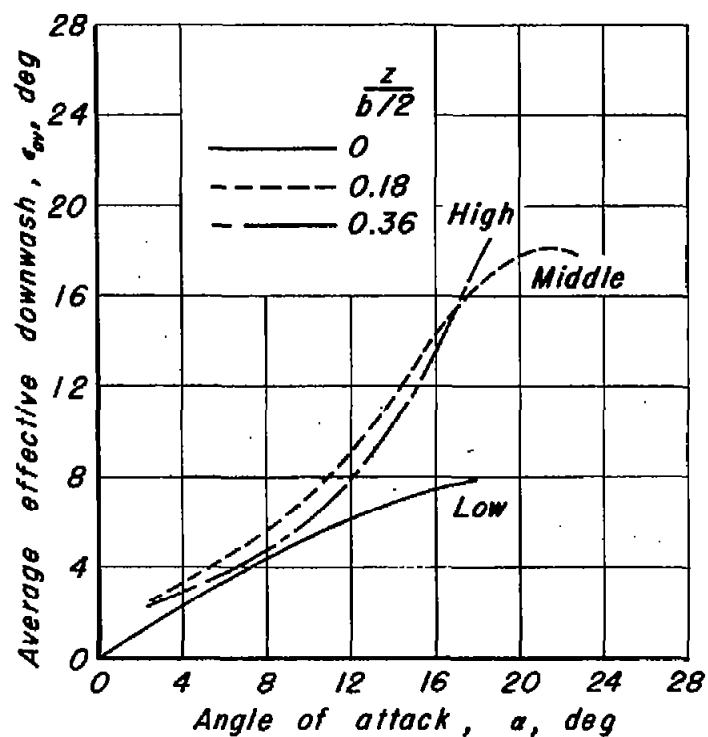
(a) Tail 1; c.g., 0.463 \bar{c} .

Figure 6.- Longitudinal characteristics of the model with the horizontal tails in the high position. $\frac{z}{b/2}$, 0.36.

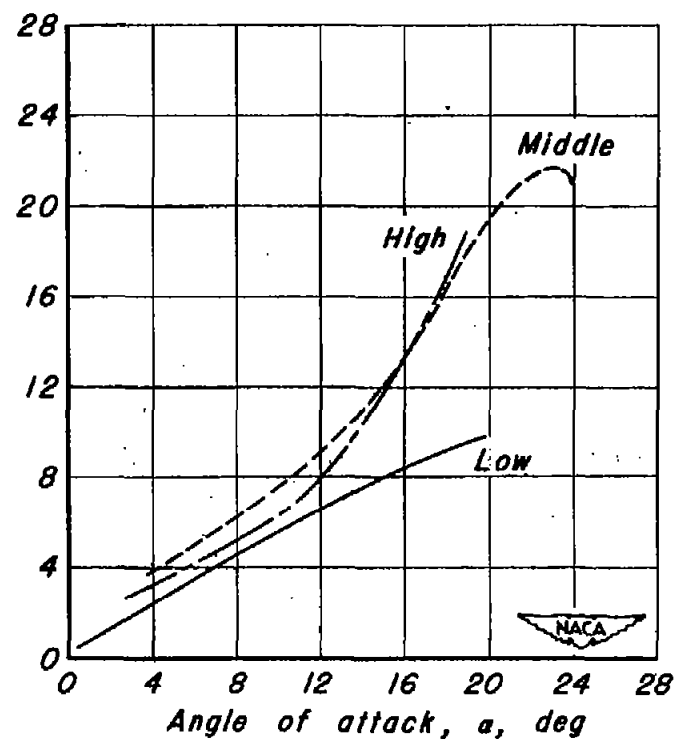


(b) Tail 2; c.g., 0.410 \bar{c} .

Figure 6.- Concluded.



(a) Tail 1.



(b) Tail 2.

Figure 7.- Variation of average effective downwash angle with angle of attack.

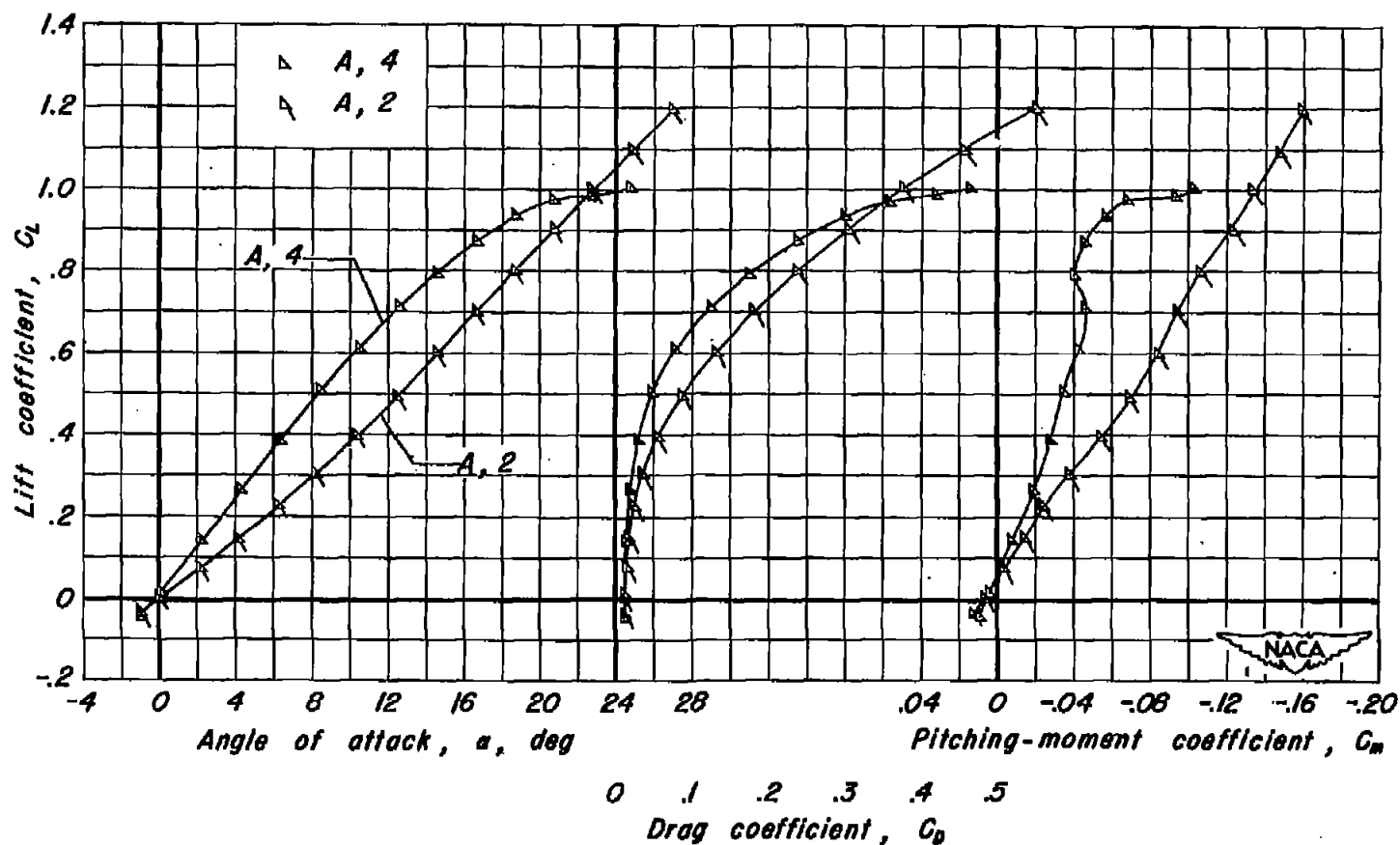


Figure 8.- Comparison of the aerodynamic characteristics of the aspect ratio 4 triangular wing-fuselage-vertical-tail configuration with the characteristics of a similar configuration having an aspect ratio 2 triangular wing; c.g., 0.250 \bar{c} .

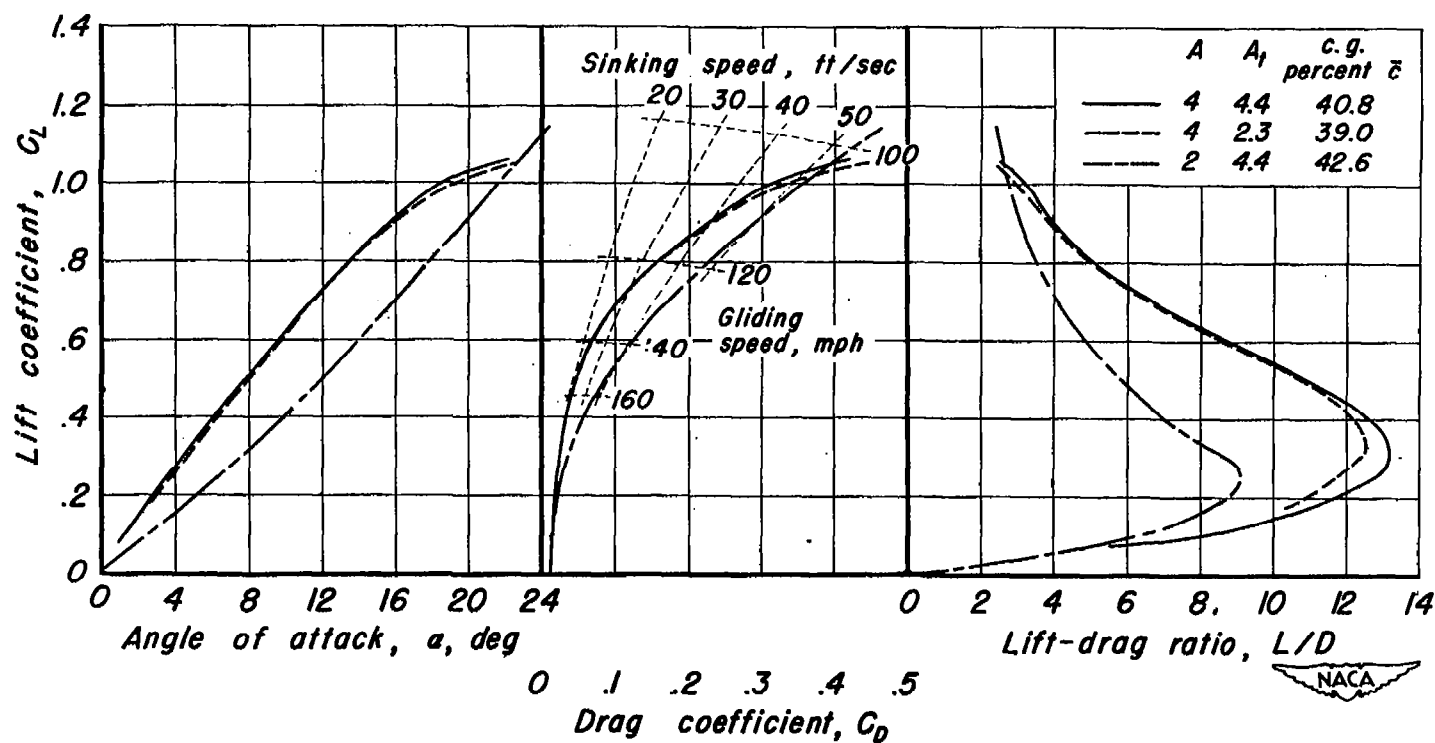


Figure 9.- Comparison of the lift and drag characteristics of trimmed, triangular-wing airplanes having aspect ratio 4 and aspect ratio 2 wings and all-movable horizontal tails. $\frac{z}{b/2}$, 0; W/S, 30 pounds per square foot.

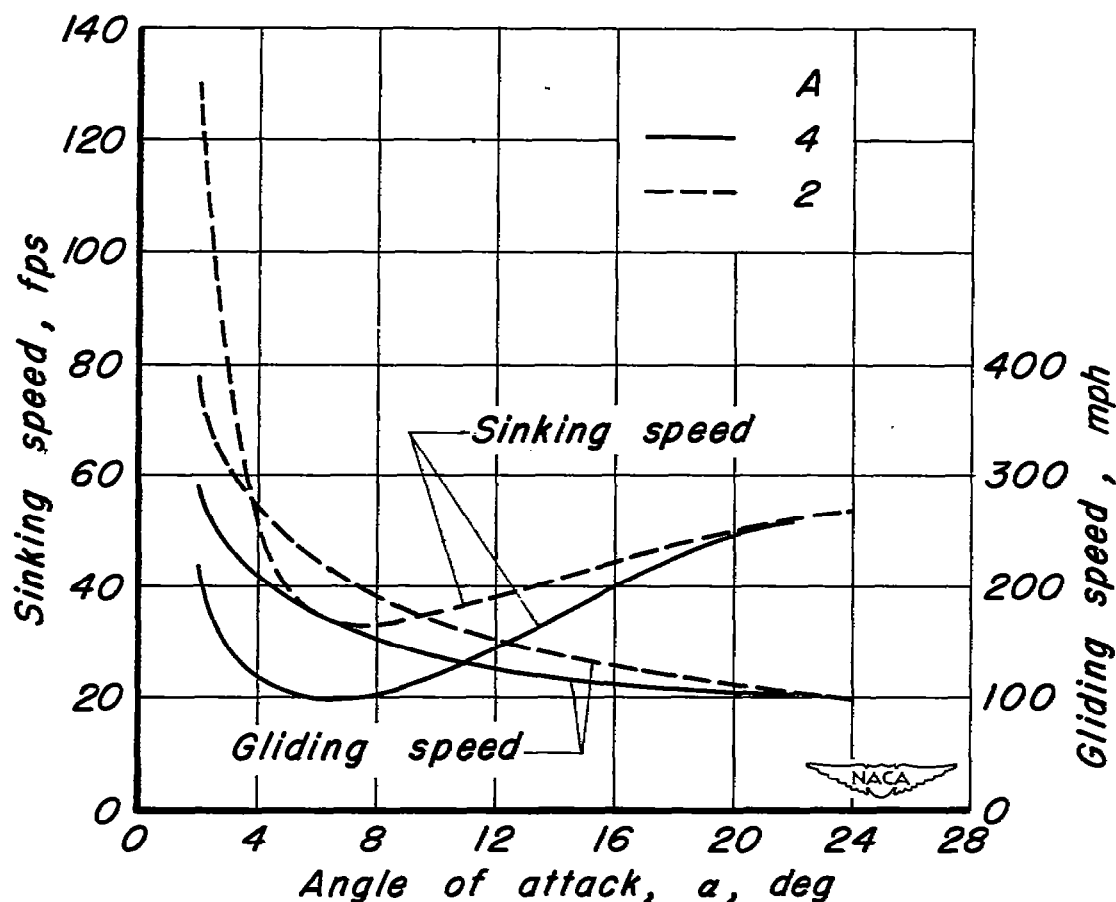


Figure 10.- The variation of gliding and sinking speeds with angle of attack for two trimmed triangular-wing airplanes with all-movable horizontal tails. A_t , 4.4; $\frac{z}{b/2}$, 0; W/S , 30 pounds per square foot.

CONFIDENTIAL



3 1176 00511 1696



CONFIDENTIAL